Journal of Ceramic Processing Research. Vol. 6, No. 4, pp. 321~325 (2005)

JOURNAL OF
Ceramic Processing Research

Fabrication and mechanical properties of fibrous silicon nitride monolithic ceramics

Hai Guo, Dae-Hyun Yoon[a] and Dong-Woo Shin[a,*]

Department of Materials Science and Engineering, Division of Ceramics, Tsinghua University, Beijing, 100084 China

[a]Ceramic Matrix Composites (CMCs) Lab. Division of Materials Science and Engineering, Engineering Research Institute, Gyeongsang National University, Jinju, Gyeongnam 660-701, Korea

Fibrous Si_3N_4 monolithic ceramics with a hexagonal cell (Si_3N_4 fiber) and diameters in the range of 0.1-0.5 mm were processed using a composite fabrication method with a high preferred orientation by the tape casting of seeds of rodlike β-Si_3N_4 single crystals. The densified Si_3N_4 fibrous monolith showed a fracture toughness of 17 MPa·m$^{1/2}$ and a three-point bend strength of 690 MPa. The application of reinforcement with SiC whiskers exhibited a fracture toughness (24 MPa·m$^{1/2}$) and strength (705 MPa). Grain orientation, interface, and reinforcement played a deciding role in mechanical properties of these monolithic ceramics.

Key words: Fibrous Si_3N_4, Fracture toughness, SiC whisker, Grain orientation.

Introduction

Reinforcement of ceramics with fibers is recognized as a new generation technique for making high performance monolithic ceramics. However, the main disadvantages associated with this technique are the expensive and complex nature of fiber processing. Coblez [1] invented a novel method to overcome this problem. His process involves spinning or extrusion of ceramic powder mixed with organic binders. The green fibers which are formed via the Coblez method are sintered to become polycrystalline ceramic fibers. The green fibers coated with interface materials acted as basic structural units to form monolithic ceramics in composite fabrication. This concept was first introduced by Baskaran and others to improve the fracture toughness in ceramics [2-5]. Preferred orientation of the grains also enhances the fracture toughness. Kyoshi et al. [6] controlled the preferred orientation through tape casting the seeds of rodlike β-Si_3N_4 single crystals to give an optimum size and distribution of elongated large grains in self-reinforced Si_3N_4 and, thus, improved the fracture toughness (K_{IC}) to 11.1 MPa·m$^{1/2}$.

The study have discusses the role of fiber diameter, and the interface and incorporation of toughening agents (β-Si_3N_4 and SiC whiskers) in determining the mechanical properties of fibrous Si_3N_4 monolithic ceramics.

Experimental Procedures

The process of fibrous monolithic ceramics is sketched in Fig. 1. This study used β-Si_3N_4 seeds which were prepared by heating powder of 90 wt% α-Si_3N_4, 7 wt% Y_2O_3 and 3 wt% Al_2O_3 at 1650 °C for 1.5 h under a nitrogen pressure of 0.5 MPa [7]. Synthesized seeds consist of rodlike β-Si_3N_4 single crystals with a mean diameter of 0.5 μm and a length of 4.0 μm. Green fibers were extruded using a plastic mixture of 12 wt% poly (vinyl) alcohol (PVA) as the organic binder, 3 wt% glycerol as the plasticising agent, 55 wt% ball-milled mixture of α-Si_3N_4 (Founder Corporation, Beijing, China), 7 wt% Y_2O_3 (purity >99.9%, Hokke Chemicals, Tokyo, Japan), 3 wt% Al_2O_3 (purity >99.9%), and 20 wt% SiC whickers (TWS-400, Hokke Chemicals, Tokyo, Japan) or 3 wt% β-Si_3N_4 seeds (in this case, 72 wt% of α-Si_3N_4 was used). Green fibers extruded with different fiber diameters were subsequently coated with 75 wt% BN and 25 wt% Al_2O_3 slurry. The coating thickness was ~40 mm (Fig. 2). These green fibers were cut and stacked in a particular order in a graphite die. Heat treatments at 260 °C for 2 h and at 400 °C for 4 h were given to remove the organic binder. Subsequently, the green body was hot pressed at 1800 °C for 1 h under a nitrogen atmosphere to form a fibrous monolithic Si_3N_4.

The microstructure of the fibrous monolithic ceramics was examined using SEM (CSM950, OPTON, Germany). Flexural strength was measured with a span of 30 mm

*Corresponding author:
Tel : +82-55-751-5332
Fax: +82-55-755-6755
E-mail: dwshin@gsnu.ac.kr

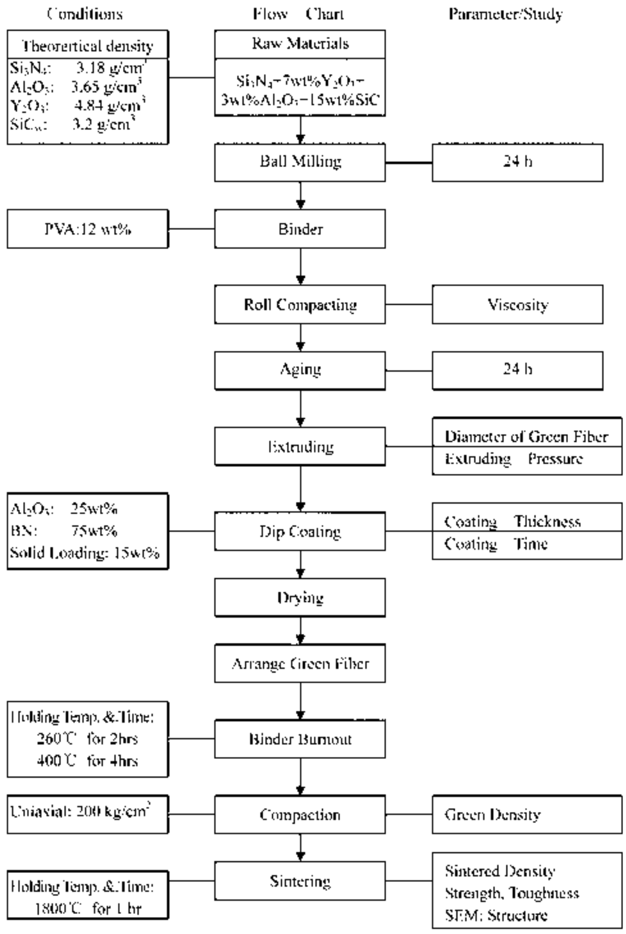

Fig. 1. Flow chat describing fabrication procedure of fibrous monolithic Si_3N_4 ceramics.

and crosshead speed of 0.5 mm/minute at room temperature. The fracture toughness was determined by the single-edge-notch-beam method at room temperature with a crosshead speed of 0.05 mm/minute. Specimens for mechanical testing were sliced parallel to the fiber direction into test bars (3×4×32 mm^3 for bending strength and 4×6×32 mm^3 for fracture toughness).

Results and Discussion

Microstructure of Fibrous Monolithic Ceramics

The microstructure of synthesized Si_3N_4/BN-Al_2O_3 fibrous monolithic ceramics is shown in Fig. 3. Scanning electron micrographs (Fig. 3(a) and (b) show the planes parallel to the fiber direction while Fig. 3(c) shows the “end view” of the uniaxially aligned fibers). The cross section of fibers is identical to the hexagonal cross section of the green fibers rather than a circular cross section. The interface materials BN-Al_2O_3 form a weak interface with the fibers. Figure 4 shows a SEM micrograph of the structure of Si_3N_4 fibrous cell. The one-dimensional orientation of elongated grains and whiskers reveals the preferred orientation of self-sintered Si_3N_4.

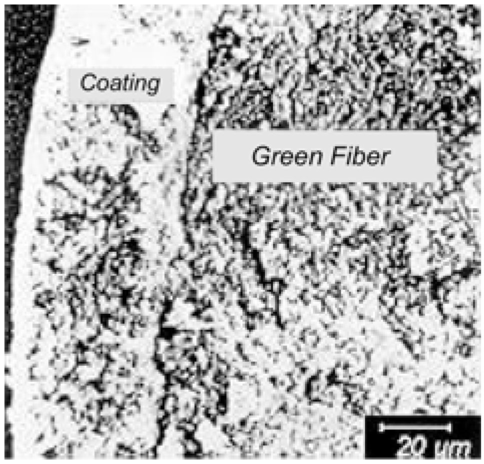

Fig. 2. SEM micrograph of Si_3N_4 green fiber with BN-Al_2O_3 coating.

Mechanical Properties of Fibrous Monolithic Ceramics

The mechanical properties of fibrous monolithic Si_3N_4 with seeds of whiskers are summarized in Table 1. It is found that the diameter of the green fiber plays a vital role in deciding the mechanical properties (Fig. 5). A decrease in diameter of green fibers leads to a decrease in the size of the basic structural unit and limits the propagation of cracks to a smaller field. Similarly an increase in the extent of the weak interface in the monolithic ceramic is expected with a decrease of the green-fiber diameter. This enhances the absorption of crack propagation energy and consequently improves the K_{IC}. The increase in weak interface, however, diminishes the strength of the ceramic. In order to improve the strength, whisker reinforcement was used. The addition of whiskers obstructs the propagation of cracks, and the result is a stronger basic structural unit.

The load-deflection curve for this system is shown in Fig. 6. The fibrous monolithic ceramic shows failure in flexure but in a noncatastrophic manner. The load, which leads to crack formation and breaking of ceramics, increases with a decrease in diameter of the green fibers. The apparent work-of-fracture evaluated from the load-deflection curve reaches a potential level of 4000 J/m^2, which leads to the formation of more reliable ceramic material.

Crack Propagation Path

Figure 7 shows a typical fracture behavior of the fibrous monolithic ceramic. The major crack deflects at the cell boundary and causes the generation of many microcracks along the cell boundaries. Crack propagation energy gets dissipated along the cell boundary, that leads to a considerable improvement in fracture toughness. Cracks are ~15 mm in width and symmetrically distributed near the center of the beam. The cracks further propagate in a stepped manner and the whisker-reinforced Si_3N_4 shows debonding and pull out as observed in Fig. 7.

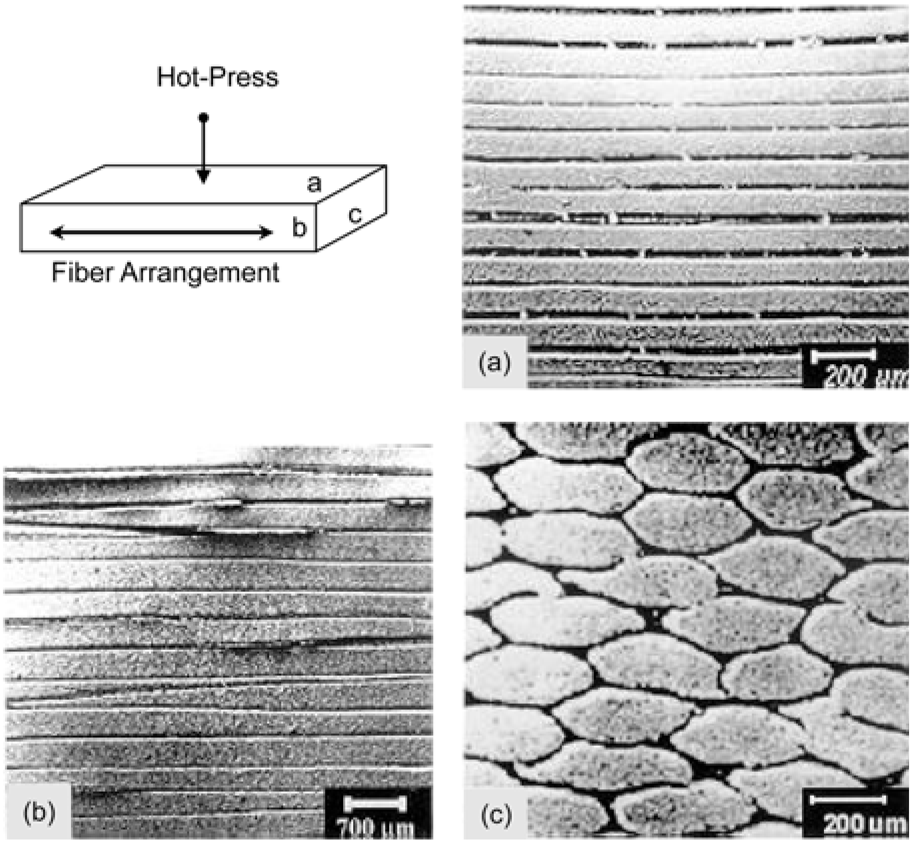

Fig. 3. SEM micrographs of macrostructure of Si_3N_4 fibrous monolithic ceramic.

Fig. 4. SEM micrograph of structure inside Si_3N_4 cells of Si_3N_4 fibrous monolithic ceramic.

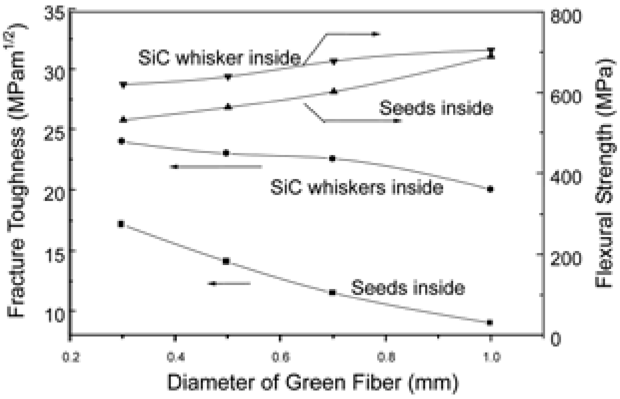

Fig. 5. Mechanical properties of Si_3N_4 fibrous monolithic ceramics.

Derivation of Equation of Fracture Toughness and Its Relation with Fiber Diameter

The microstructure of fibrous monolithic ceramics is quite similar to that of fiber-reinforced composites. Figure 8(a) shows sketch of a composite structure. Every cell has the shape of a cylinder with a diameter of r_0. The axes of these cylinders are parallel to each other and located on a set of parallel plates, and the distance between the adjacent parallel plates is h.

The application of stress (σ_z) induces tensile forces near the crack tip, both fiber and interface bear these forces [8] :

$$\sigma_Z = \frac{K_I h \sqrt{2d}}{\pi \sqrt{\pi}\, r_0^2} \tag{1}$$

where K_I is the stress intensity factor and d is the distance between the two neighboring cylinders.

Stress-induced cracks generate microcracks around the fiber surface and propagate along the interface. The length of crack propagation (L_0, also called the length of the invalid region) (shown in Fig. 9) is calculated on

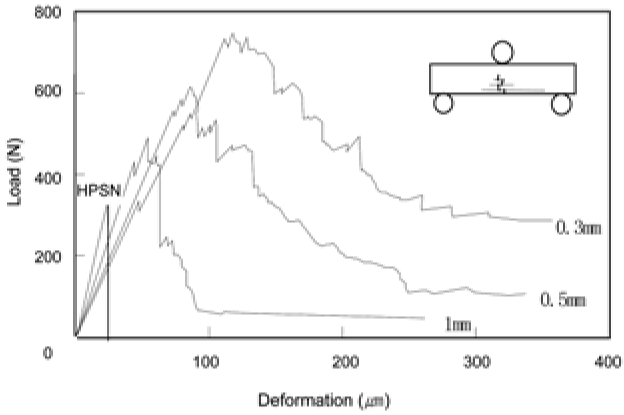

Fig. 6. Typical load-deformation curves of HP Si_3N_4 and Si_3N_4 fibrous monolithic ceramics with different diameters of green fibers.

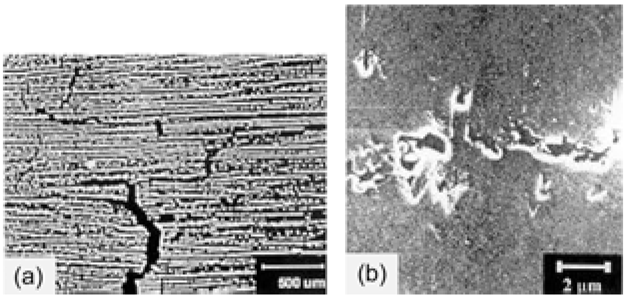

Fig. 7. SEM micrographs of crack propagation in Si_3N_4 fibrous monolithic ceramic. (a) major crack, a branch of crack can be seen, (b) crack propagation in Si_3N_4 cells, white line means the micro-crack

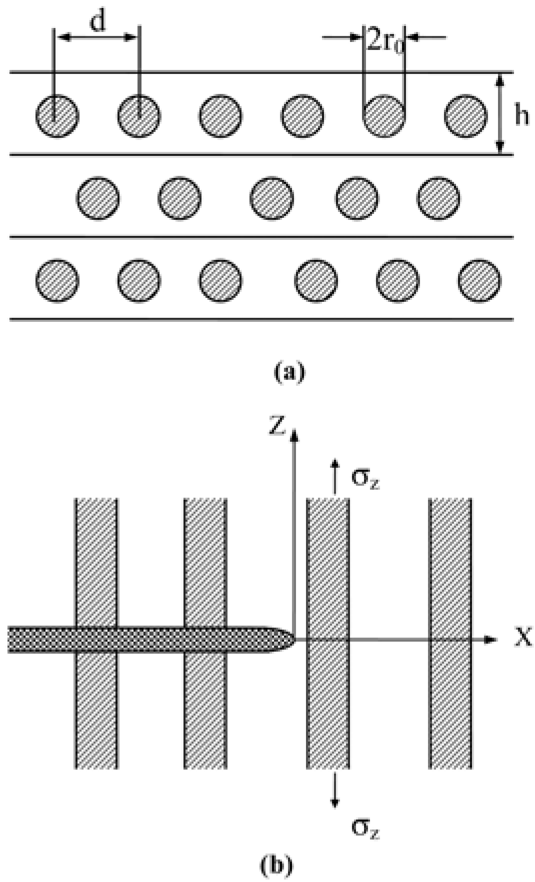

Fig. 8. Fibrous monolithic structure. (a) Macrostructure, (b) one set of fibers

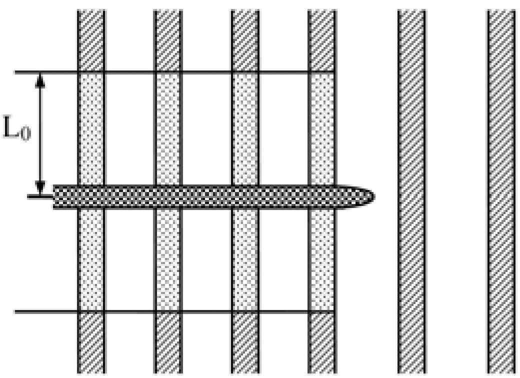

Fig. 9. Length of propagation of micro-cracks. (It is also the length of invalid region)

the basis of a quasi-brittle principle.

$$L_0 = \frac{\xi(\sigma_f) r_0^{3/2} \pi^{3/4}}{4\sqrt{6}\,\eta f_v^{1/4} K_{XC}} \qquad (2)$$

where $\xi(\sigma_f)$ is a function related to σ_f, the flexural strength of the fiber, η is a structural constant, and V_f is the volume percent of fibers.

Application of stress causes the strain in the bulk structure. The strain release energy (γ) is given by :

$$\gamma = \gamma_f v_f + 2\pi r_0 L_0 n \gamma_{fi} \qquad (3)$$

where γ_f is the fiber strain energy release rate, γ_{fi} is the interfacial strain energy rate, and n is the number of

Table 1. Mechanical properties of Si_3N_4 fibrous monolithic ceramics

Diameter of Green Fibers D (mm)	3 wt% β-Si_3N_4 Seeded		15 wt% SiC Whisker Contained	
	Flexural Strength σ_f (MPa)	Fracture Toughness K_{IC} ($MPa{\cdot}m^{1/2}$)	Flexural Strength σ_f (MPa)	Fracture Toughness K_{IC} ($MPa{\cdot}m^{1/2}$)
1.0	698±68	8.98±1.04	705±71	20.01±1.17
0.7	602±61	11.52±0.98	678±62	22.56±1.01
0.5	562±51	14.11±1.00	639±60	22.96±0.88
0.3	530±42	17.16±1.02	619±47	23.95±0.92

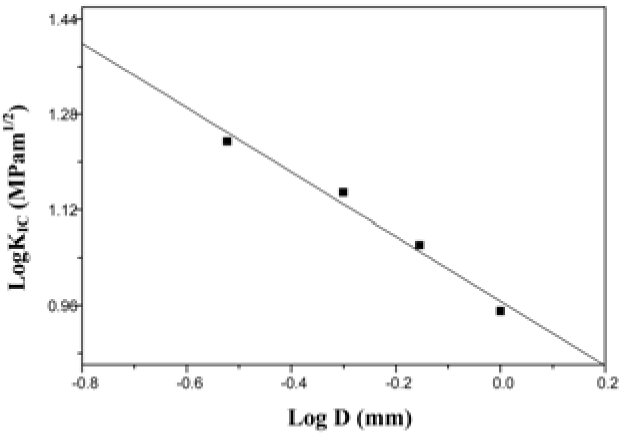

Fig. 10. Logarithmic curve of fracture toughness and the diameter of green fibers and the points are the experiment dates.

fibers in each unit volume. In the fibrous monolithic ceramic, fibers are packed so closely that the thickness of the boundary (interface) can be ignored, so :

$$n = V_f / \pi r_0^2 \tag{4}$$

We can ignore the first term of Eq. (3) because L_0 is much larger than r_0, so we can rewrite Eq. (3) as :

$$\gamma = 2\gamma_{fi} V_f \frac{L_0}{r_0} \tag{5}$$

Using the relationship between the strain energy release rate and the fracture toughness, we get :

$$K_{IC} = \sqrt{2E\gamma} = \sqrt{4E\gamma_{fi} \cdot V_f \frac{L_0}{r_0}} \tag{6}$$

where E is Young's modulus. The validity of Eq. (6) in the case of fibrous ceramics is examined using the properties of fibrous monolithic Si_3N_4 obtained in the present investigation. Fibrous monolithic Si_3N_4 having 15 wt% SiC whiskers with a 0.3 mm fiber diameter has a 15 mm broken region width (which equals $2L_0$) resulting in E=411 GPa, and γ_{fi}=10 J/m^2, and V_f= 77.9%. Substitution of these parameters into Eq. (6) gives a K_{IC}=25.31 MPa·m$^{1/2}$. While the experimental value is 23.95 MPa·m$^{1/2}$ (shown in Table 1), the deviation is in the permissible range, <10%.

Equation (6) also expresses the relation of fracture toughness with fiber diameter, :

$$K_{IC} = 9.267D^{-0.5198} \tag{7}$$

where D is the diameter of the green fibers. Experimental values of K_{IC} shown in Fig. 10 are in close proximity with the curve based on the theoretical values calculated used Eq. (7).

Conclusions

This investigation concludes that (1) Incorporation of β-Si_3N_4 seeds or SiC whiskers improves the fracture toughness of fibrous monolithic Si_3N_4 ceramics; and (2) The fiber diameter plays a deciding role in the mechanical properties: The smaller the diameter of the green fiber, the higher the mechanical properties of the ceramic are.

Acknowledgement

This work was supported by the Japan-Korea Core University Program entitled "New Processing and Nano-structure/Property Relationship of Multi-functional Ceramic Materials"

References

1. W.S. Coblenz, U.S. Patent 4772524, 20[9] (1988).
2. S. Baskaran, S.D. Nunn, and J.W. Halloran, J. Am. Ceram. Soc. 76[9] (1993) 2217-24.
3. S. Baskaran and J.W. Halloran, J. Am. Ceram. Soc. 76[9] (1993) 2225-32.
4. S. Baskaran and J.W. Halloran, J. Am. Ceram. Soc. 77[5] (1994) 1249-55.
5. S. Baskaran and J.W. Halloran, J. Am. Ceram. Soc. 77[5] (1994) 1256-62.
6. Kiyoshi Hirao, M. Ohashi and M.E. Brito, J. Am. Ceram. Soc. 78[6] (1995) 1687-90.
7. Kiyoshi Hirao, T. Nagaoka and M.E. Brito, J. Am. Ceram. Soc. 77[7] (1994) 1857-62.
8. K.Z. Huang, Mechanism of engineering brittle materials, Sicence Press, Beijing. China, (1990) 472-484.